

**Iowa State University**

---

**From the Selected Works of Valery I. Levitas**

---

2006

# Kinetics of Strain-Induced Structural Changes under High Pressure

Valery I. Levitas, *Texas Tech University*

Oleg M. Zarechnyy, *Texas Tech University*



Available at: [https://works.bepress.com/valery\\_levitas/32/](https://works.bepress.com/valery_levitas/32/)

# Kinetics of Strain-Induced Structural Changes under High Pressure

Valery I. Levitas\* and Oleg M. Zarechnyy

Texas Tech University, Center for Mechanochemistry and Synthesis of New Materials,  
Department of Mechanical Engineering, Lubbock, Texas 79409

Received: March 22, 2006; In Final Form: May 30, 2006

A mechanism-based microscale kinetic theory for strain-induced structural changes (SCs) (that includes phase transformations (PTs) and chemical reactions (CRs)) is developed. Time is not an independent parameter in this theory; instead, plastic strain is a time-like parameter. Kinetics depends essentially on the ratio of the yield strengths of phases. Stationary and nonstationary solutions of the kinetic equations are analyzed for various cases, including SCs between two phases in an inert matrix and between three phases in silicon and germanium. A number of experimental phenomena are explained, and material parameters controlling the kinetics of strain-induced SCs are determined. This includes the possibility of intensification (or suppression) of SCs at the initial stage of straining by adding a stronger (or weaker) inert phase, zero pressure hysteresis that however has nothing to do with phase equilibrium pressure, the possibility of obtaining some phases (that cannot be obtained under hydrostatic loading) under strains, and the possibility to obtain some phases under relatively small shear, which disappear under larger shear.

## I. Introduction

In addition to SCs caused by temperature and/or pressure, there is a broad class of SCs induced by plastic straining. Strain-induced synthesis of various materials and chemical compounds (superhard, amorphous, and semiconducting) by ball-milling (mechanical alloying or mechanosynthesis) is one of the most important technological examples.<sup>1,2</sup> Interpretation of geophysical experiments (e.g., deep earthquakes,<sup>3–5</sup> ignition of explosives,<sup>6–8</sup> and friction and wear data<sup>9</sup>) requires understanding of shear-induced SCs, in particular, in shear bands. Fundamental experimental aspects of strain-induced SCs are extensively studied under high pressure. Starting with the pioneering work by Bridgman<sup>10</sup> on rotating cemented carbide anvils, followed by the work on rotational diamond anvils by Blank's group,<sup>11–16</sup> it is well-known that the addition of plastic shear, through the rotation of one of the anvils, leads to findings that have both fundamental and applied significance and do not have counterparts in pressure/temperature-induced SCs. Thus, plastic shear leads to a significant (in some cases, by a factor of 3–5) reduction of PT<sup>12,13</sup> and CR<sup>17,18</sup> pressure. It also leads to the formation of new phases, which were not produced without rotation.<sup>17–22</sup> The most important point for the current study is that the volume fraction of the product phase or the reaction product is an increasing function of the plastic shear strain<sup>12,13,17,18</sup> and is independent of time. Therefore, strain-controlled (rather than time-controlled) kinetics is considered. Plastic shear reduces pressure hysteresis, i.e., the difference between the start pressure of direct and reverse PT.<sup>11,23</sup> This led to the hope that plastic shear could be used to localize the phase equilibrium pressure. In one case, pressure hysteresis was reduced to zero; from this, it was claimed that the obtained PT pressure could be interpreted as an equilibrium pressure.<sup>11</sup> As we will show, this is not true. In another case, the possibility of intensification (or suppression) of CRs by adding a stronger (or weaker) inert phase was observed experimentally.<sup>17,18</sup>

Despite the fundamental and applied importance of the effect of plastic shear on SCs, until recently, there were no efforts to

explain this effect theoretically. Zharov<sup>17,18</sup> suggests the simplest formal strain-controlled kinetic equations that can be fitted to experiment for specific reactions. Gilman's<sup>24,25</sup> qualitative atomistic models are focused on the effect of elastic rather than plastic shear. Recently, we developed a theory describing the strain-induced SCs at the macroscale<sup>26,27</sup> (plastic flow of a sample with SC), at the microscale<sup>28</sup> (strain-controlled kinetic equations), and at the nanoscale<sup>29</sup> (nucleation at a dislocation pileup). Our combined multiscale theory<sup>30,31</sup> explains fifteen mechanochemical phenomena.

The mere fact that the above phenomena are observed for PTs and CRs in various classes of materials suggests that there are some universal microscopic (on the scale of 1–1000 nm) explanations for their existence, independent of specific atomistic and nanoscale mechanisms of SC. In this paper, we develop and comprehensively study some general aspects of the mechanism-based microscale kinetic theory of strain-induced SCs.

In section II, we summarize the main universal nanoscale features of the nucleation at the strain-induced defects (dislocations, dislocation pileup, or various tilt boundaries) that can be transferred into microscale kinetic equations. In section III, the kinetic equations for an  $n$ -phase system are derived and analyzed. This model allows us to describe some known experimental phenomena and understand which material parameters control the kinetics of strain-induced SCs. Distinguished features of the new kinetic equations include the following:

(a) The equality of the driving forces for SCs to zero does not determine the relationship between phase equilibrium pressure and temperature; instead, they result in strain-controlled kinetic equations. The phase equilibrium pressure (or temperature) does not participate in kinetic equations and consequently cannot be determined from them.

(b) Time is not an independent parameter. Instead, plastic strain is a timelike parameter, i.e., derivatives are evaluated with respect to accumulated plastic strain rather than time. That is

why we call this kinetics strain-controlled rather than time-controlled.

(c) Kinetics depends essentially on the mechanical properties of phases, namely, on the ratio of the yield strengths of phases.

(d) This dependence also involves the volume fraction of phases which changes the order of the kinetic equations. In the general case, the order of the reaction is not determined.

Explicit stationary solutions are derived for three-phase systems, and their dependence on the ratio of the yield strengths of phases is analyzed.

In section IV, SCs between two phases in an inert matrix are studied. Both stationary and nonstationary solutions are obtained and analyzed for several pressure ranges. The nonstationary solutions explain the possibility of intensification (or suppression) of SCs by adding a stronger (or weaker) inert phase, which was observed experimentally.<sup>17,18</sup> However, such an intensification (suppression) is effective only at the initial stage of the SC. Stationary concentration of the product phase is independent of the inert matrix but can be reached at smaller plastic strains. Section IV also explains zero-pressure hysteresis observed in ref 11. It is demonstrated that it has nothing to do with phase equilibrium pressure. At the initial stage of deformation, our equation results in a linear relationship between the volume fraction and the plastic strain observed for a number of CRs.<sup>17,18</sup>

In section V, stationary and nonstationary solutions for strain-induced PTs between three phases in Ge and Si are studied numerically and used to derive some general consequences. Results demonstrate how phases that cannot be obtained under hydrostatic loading could be obtained under applied strains. It is also found that, while one of the phases can be obtained in an experimentally detectable quantity under relatively small shear, it almost disappears under larger shear.

Despite the fact that the constants in kinetic equations cannot currently be determined experimentally, some experimental phenomena are described, and a number of useful conclusions are derived from our analysis. These results are important especially from the point of view of the search for new strain-induced phases. In addition, the effect of the yield strength of phases on SC kinetics is analyzed. Our model provides methods of characterization and control of strain-induced SCs. These methods can be used to obtain and intensify SCs, which were not obtained otherwise, e.g., leading to metallic hydrogen.<sup>32–34</sup>

## II. Main Features of Strain-Induced Nucleation Mechanism

We will summarize some of the results of nanoscale modeling of strain-induced SCs<sup>29–31</sup> which will be necessary for our study. For CR, plastic flow produces a fragmentation, strain-induced diffusion, and mixing of components at the same level as in liquid-phase CR;<sup>17,18</sup> that is why mixing will not be considered as the limiting factor. This will allow us to use the same approach for both PTs and CRs. There is a fundamental difference between pressure-induced SCs and strain-induced SCs under high pressure. Pressure-induced SCs occur predominantly at existing defects (e.g., dislocations, point defects, grain and twin boundaries, stacking faults) which represent stress (pressure) concentrators. Thus, the number of nucleation sites is limited. That is why one has to increase pressure to activate less potent defects. The strain-induced nucleation occurs at new defects permanently generated during plastic flow. That is why it is possible to increase local stresses and promote the SCs near the new defects by increasing plastic shear at constant pressure. Stress concentration near the defects significantly

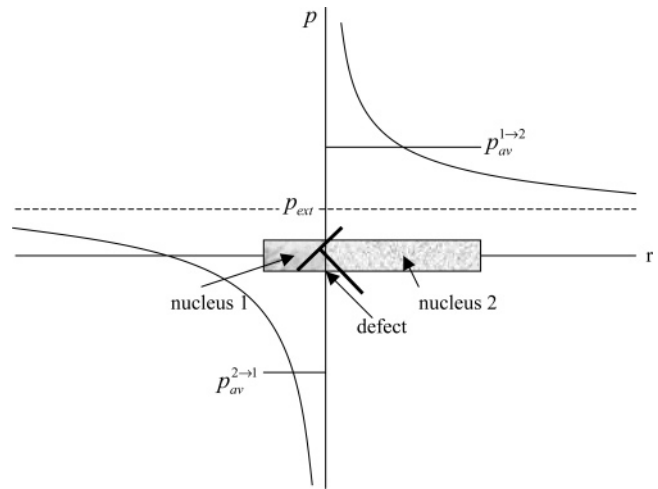


**Figure 1.** Nucleation on a typical strain-induced defect that appears during the small prescribed strain increment  $\Delta q_i$ . The resultant pressure (curves in the figure) is a superposition of the external pressure,  $p_{ext}$ , and the pressure (in general stress) field of the defect. The stress field of the defect has different senses from both sides of the defect, and its magnitude reduces away from the defect. A nucleus of phase 2 within phase 1 and a nucleus of phase 1 within phase 2 appear simultaneously. The transformation work is proportional to the area enclosed between the resultant pressure and the defects;  $p_{av}^{1-2}$  and  $p_{av}^{2-1}$  are the pressures averaged over the nucleus that produce the same transformation work. The larger the volume of the nucleus  $V_n^{ij}$  (and consequently  $\Delta c_j = V_n^{ij}/V$ ) is, the smaller the stress and the transformation work averaged over the  $V_n^{ij}$  is. Consequently, the transformation work decreases with increasing  $(\Delta c_j)/(\Delta q_i) = (dc_j)/(dq_i)$ .

increases the driving force for the SC and can cause SCs at significantly lower external pressure, thus contributing to the overall SC kinetics. Stress singularity near the defect effectively reduces the nucleation barrier due to surface energy and for strong enough defects (singularities) leads to barrierless nucleation, which does not require thermal fluctuations. This explains the relatively low-temperature sensitivity of strain-induced SCs, as well as the strain-controlled rather than time-controlled kinetics. Because of this, time is not an essential independent variable, and strain plays a role of timelike parameter. Indeed, the prescribed strain increment generates defects (dislocation pileups, various tilt boundaries, shear-band intersections, grain, twin, and subgrain boundaries, and stacking faults) with barrierless (i.e., very fast) nucleation and growth of the product phase up to the size where stress concentration is reduced and cannot drive the interface further (Figure 1). For the typical experimental observation time of the few second range, this resembles instantaneous SC. As straining stops, no new defects or nuclei appear, and the growth of the existing nuclei is thermodynamically impossible. As the contribution of the stress concentration to the driving force for SC in a finite volume is finite, the lowest possible pressure,  $p_e^j$ , exists, below which strain-induced SC from the low-pressure phase  $i$  to the high-pressure phase  $j$  is undetectable. An additional important point is<sup>29–31</sup> that defects generate both compressive and tensile pressures (stresses), which are of the same magnitude, e.g., for dislocations (Figure 1) and dislocation pileups. Consequently, similar defects produced in the product phase will increase the driving force for the reverse SC. Thus, defects simultaneously promote both direct and reverse SCs in different regions. Furthermore, plastic strain is distributed heterogeneously in a multiphase material. For example, for a two-phase mixture 1 + 2, the stronger phase 1 is, the smaller the fraction of the

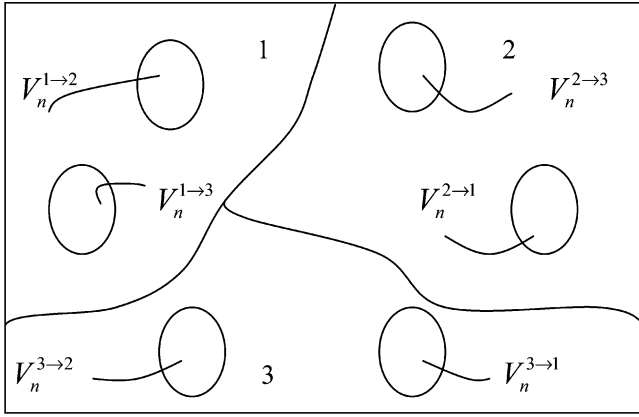


**Figure 2.** Scheme of structural changes in three-phase model.

plastic strain concentrated within it is, and the larger the prescribed (external) plastic shear is required to be to cause the SCs.

The results discussed above represent basic nanoscale reasons for the mechanochemical phenomena that are of interest in this paper. All of these results will be conceptually incorporated in the microscale model.

### III. Thermodynamically Consistent Strain-Controlled Kinetic Equation for Structural Changes

**Thermodynamic Criterion for Structural Changes.** We will consider a representative volume  $V$  consisting of  $n$ -phase material; each phase  $i$  can generally be transformed into any other phase  $j$ ; simultaneously, phase  $j$  can be transformed into  $i$  but with a different rate (Figure 2). If SC between some phases is impossible, we will set the corresponding transformation rates equal to zero. General theory of SCs in inelastic materials is developed in refs 35 and 36 and summarized in ref 30. For solid–solid SC, the transformation strain tensor,  $\epsilon_t$ , transforms an infinitesimal volume or a unit cell of the stress-free parent phase into a unit cell of the stress-free product phase. In the case of CR, both materials, before and after the CR, can consist of several substances. For brevity, we will use the term “phases” in this case as well. We neglect all internal atomic displacements (e.g., shuffles) inside the volume under consideration.

We will describe plastic deformation averaged over the volume  $V$  in terms of equivalent plastic strain  $q$  (Odqvist parameter). By definition, the Odqvist parameter  $q$  is the scalar path-dependent measure of plastic strain determined by the equation  $\dot{q} := (2\mathbf{d}_p : \mathbf{d}_p/3)^{1/2}$  (see, e.g., ref 37 or any textbook on plasticity theory), where  $\mathbf{d}_p$  is the plastic strain rate tensor,  $:=$  is equal by definition, and  $:$  means double contraction of tensors. For example, for pure compression (tension),  $q = \ln|h/h_0|$ , where  $h$  and  $h_0$  are current and initial lengths of the sample. For simple shear,  $\dot{q} = \gamma/\sqrt{3}$  with  $\gamma$  for shear strain. For combined compression and shear,  $\dot{q} = \sqrt{(\dot{h}/h)^2 + \dot{\gamma}^2/3}$ , and  $q$  depends on the loading path.<sup>30,31</sup> Similarly, plastic strain in the  $i$ th phase will be characterized by the Odqvist parameter  $q_i$  averaged over the phase  $i$ . The goal of this section is to derive a strain-controlled kinetic equation  $dc_i/dq = f(p, c_j)$  for the volume fraction of each phase  $i$ , where  $p$  is the macroscopic pressure applied to the volume  $V$ . Since the SCs represent a sequence of nucleation events without further growth and time is not an explicit parameter, kinetic equations have to be derived using the thermodynamic criterion eq 1 for the appearance of each strain-induced nucleus and the averaging procedure.<sup>29–31</sup> This

is an extremely complex procedure. To obtain a simple analytical expression, we approximate the microscopic transformation work averaged over the transforming volume  $V_n^{i \rightarrow j}$  (Figure 2) by some decreasing function of  $dc_j/dq_i$  (eq 4). Validity of such an approximation follows from our analysis of nucleation at arbitrary strain-induced defects (Figure 1) as well as an analytical solution for nucleation at dislocation pileup<sup>29–31</sup> and finite element modeling of nucleation at shear band intersection.<sup>38</sup> Resolving the thermodynamic SC condition for  $dc_j/dq_i$ , we obtain a strain-controlled kinetic equation (eq 5) for SC  $i \rightarrow j$ . In a similar way, a kinetic equation for the reverse SC  $j \rightarrow i$  can be derived (eq 6). In the next step, we express the strain in each phase  $q_i$  via the prescribed strain  $q$  and the yield stresses  $\sigma_{yk}$  of all phases (eq 8). Algebraically adding the rates of  $i \rightarrow k$  and  $k \rightarrow i$  SCs for all  $k \neq i$  and taking into account the expression  $q_k(q, \sigma_{yj})$  (eq 8), one obtains the final system of kinetic eq 11 for  $dc_i/dq$ .

In the simplest case, when the temperature  $\theta$  is fixed and homogeneous in a transforming volume and the change in elastic moduli is neglected, the criterion for barrierless (athermal) SC  $i \rightarrow j$  in the multiconnected volume  $V_n^{ij}$  of an elastoplastic material is<sup>35,36</sup>

$$X_{ij} = \frac{1}{V_n^{ij}} \int_{V_n^{ij}} \int_0^{\epsilon^{ij}} \mathbf{T} : d\epsilon_t^{ij} dV_n^{ij} - \Delta\psi_{ij}(\theta) = K_{ij} \quad (1)$$

Here,  $X_{ij}$  is the driving force for SC  $i \rightarrow j$ , which represents the calculated dissipation increment due to SC only (i.e., excluding plastic dissipation) during the entire transformation process in the volume  $V_n^{ij}$  averaged over the transforming region  $V_n^{ij}$ ;  $K_{ij}$  is the actual dissipation due to SC related to interaction of a moving interface with various defects, e.g., point defects (solute and impurity atoms, vacancies), dislocations, grain, subgrain, and twin boundaries, and precipitates, as well as to the emission of acoustic waves and Peierls barrier;  $\mathbf{T}$  is the local stress tensor;  $\Delta\psi_{ij}$  is the jump in the thermal part of the free energy;  $\mathbf{T} : d\epsilon_t = \sum_{k=1}^3 T_{kl} d\epsilon_{t(kl)}$  is the incremental transformation work. For elastic materials, the expression for  $X_{ij}V_n^{ij}$  coincides with the change in Gibbs energy of the whole system.<sup>35</sup> The stress can be decomposed into a sum of the macroscopic pressure  $p$ , which is homogeneous in a representative volume  $V \gg V_n^{ij}$ , and the microscopic heterogeneous contribution,  $\tilde{\mathbf{T}}$ :  $\mathbf{T} = p\mathbf{I} + \tilde{\mathbf{T}}$ , where  $\mathbf{I}$  is the unit tensor. Since  $V$  is much larger than  $V_n^{ij}$ , the variation of  $p$  is negligible during a small SC increment. Macroscopic shear (deviatoric) strength is limited by the yield strength, which is smaller than  $p$  by a factor of  $2R/h \approx 10–100$  in the rotational diamond anvil cell experiments<sup>30,31</sup> ( $R$  and  $h$  are the radius of the anvil and the current thickness of the disk sample). We will neglect it and obtain from eq 1

$$X_{ij} = p\epsilon^{ij} + \frac{1}{V_n^{ij}} \int_{V_n^{ij}} \int_0^{\epsilon^{ij}} \tilde{\mathbf{T}} : d\epsilon_t^{ij} dV_n^{ij} - \Delta\psi_{ij} = K_{ij} \quad (2)$$

where  $\epsilon^{ij}$  is the volumetric transformation strain. To evaluate the integral in eq 2, knowledge of the specific mechanism of the strain-induced nucleation is required, and the corresponding boundary–value problem must be solved either analytically or numerically. For example, the nucleation at dislocation pileup was treated analytically in previous studies.<sup>29–31</sup> Nucleation at the shear–band intersection in TRIP steel was investigated in our paper<sup>39</sup> using a finite element solution. However, such solutions (especially if expanded for multiple defects) are too complex to study the main microscopic features of strain-

induced kinetics. In addition, such solutions require that the number of parameters be known (e.g., type and geometry of the defect, defect concentration and distribution). Therefore, we have to find the main property of the nanoscale model that can be approximately transmitted to the microscale. One of the results which can be extracted from this investigation is that there is a significant decrease in the transformation work with the ratio  $\Delta c_j/\Delta q_i \cong dc_j/dq_i$ , where  $\Delta c_j$  is a small increment of the volume fraction of a strain-induced  $j$  phase that appeared within the  $i$  phase due to the small accumulated plastic strain increment in the  $i$  phase  $\Delta q_i$ .

Qualitatively, this has to be the case for any mechanism of nucleation due to strain-induced defects. Indeed, if a single defect appears during the prescribed small strain increment  $\Delta q_i$ , its stress field reduces with an increasing distance from the defect tip (Figure 1). As the volume of the nucleus  $V_n^{ij}$  (and consequently,  $\Delta c_j = V_n^{ij}/V$ ) increases, the stress and the average transformation work over the  $V_n^{ij}$  decreases.

Thus, the main property of any nanoscale mechanism of strain-induced nucleation is that the transformation work is a decreasing function of  $dc_j/dq_i$ . We will use the following to approximate such a function:

$$\frac{1}{V_n^{ij}} \int_{V_n^{ij}} \int_0^{\epsilon^{ij}} \tilde{\mathbf{T}} : d\epsilon_t^{ij} dV_n^{ij} = \Delta X_{ij} \left[ 1 - \frac{a_{ij} (dc_j/dq_i)^{1/m_{ij}}}{c_i^{\zeta_{ij}}} \right] \quad (3)$$

Here,  $\Delta X_{ij}$  is the maximum nanoscale contribution to the transformation work for an infinitesimal nucleus, and  $a_{ij}$ ,  $\chi_{ij}$ , and  $\zeta_{ij}$  are parameters. The factor  $c_i^{\zeta_{ij}}$  takes into account that SC  $i \rightarrow j$  occurs in phase  $i$  only; therefore, if the parent phase disappeared ( $c_i = 0$ ), then  $dc_j/dq_i = 0$  as well. Substituting eq 3 in eq 2, we obtain the following microscopic criterion for SC  $i \rightarrow j$  averaged over the representative volume  $V$ :

$$X_{ij} = p \epsilon^{ij} - \Delta \psi_{ij} + \Delta X_{ij} \left[ 1 - \frac{a_{ij} (dc_j/dq_i)^{1/m_{ij}}}{c_i^{\zeta_{ij}}} \right] = K_{ij} \quad (4)$$

We will define the pressure  $p_h^{ij}$  under which SC occurs under hydrostatic loading without a strain-induced contribution by the equation  $p_h^{ij} \epsilon^{ij} - \Delta \psi_{ij} = K_{ij}$ . For  $p \geq p_h^{ij}$ , SC occurs to a high-pressure phase (or for  $p \leq p_h^{ij}$ , SC occurs to a low-pressure phase), and one needs to use the traditional time-dependent kinetic equation  $\dot{c}_{ij} = f_{ij}(p, c_k, t)$  for pressure-induced SC. Including these conditions would complicate our study and will not allow us to focus on the main regularities of strain-induced SCs. For this reason, we will only consider the following two limit cases:

(a) Kinetics of pressure-induced SCs is neglected because it is much slower than kinetics of strain-induced SCs. This is the case for fast plastic straining and will be referred to as strain-dominated kinetics.

(b) Kinetics of pressure-induced SCs is considered to be instantaneous because it is much faster than kinetics of strain-induced SCs, i.e., when pressure reaches  $p_h^{ij}$ , phase  $i$  completely and instantaneously transforms to phase  $j$ . This is the case for very slow plastic straining and will be referred to as pressure-dominated kinetics.

We also define the minimal pressure  $p_\epsilon^{ij}$ , under which strain-induced SC can start at an infinitesimal rate, by the equation  $p_\epsilon^{ij} \epsilon^{ij} - \Delta \psi_{ij} + \Delta X_{ij} = K_{ij}$ . As a result, we find that  $\Delta X_{ij} = (p_h^{ij} - p_\epsilon^{ij}) \epsilon^{ij}$ .

**Kinetic Equations for Structural Changes.** Solving eq 4 for  $dc_j/dq_i$  yields a thermodynamically consistent strain-

controlled kinetic equation for  $dc_j/dq_i$  (for direct SC  $i \rightarrow j$ )

$$\frac{dc_j}{dq_i} = \left( \frac{c_i^{\zeta_{ij}}}{a_{ij} \bar{p}_{ij}} \right)^{m_{ij}} \quad \text{where } \bar{p}_{ij} := \frac{p - p_\epsilon^{ij}}{p_h^{ij} - p_\epsilon^{ij}} \quad (5)$$

For the reverse SC  $j \rightarrow i$ , one may write

$$\frac{dc_i}{dq_j} = \left( \frac{c_j^{\zeta_{ji}}}{a_{ji} \bar{p}_{ji}} \right)^{m_{ji}} \quad (6)$$

The SC  $i \rightarrow j$  occurs for  $\bar{p}_{ij} \geq 0$  only; for  $\bar{p}_{ij} < 0$ , we can assume  $a_{ij} \rightarrow \infty$  or multiply eq 5 by the Heaviside unit step function  $H(\bar{p}_{ij})$  ( $H(x) = 1$  for  $x \geq 0$ ;  $H(x) = 0$  for  $x < 0$ ). For  $p_h^{ij} > p_\epsilon^{ij}$ , the SC occurs from the low-pressure to the high-pressure phase and  $p \geq p_\epsilon^{ij}$ . For  $p_h^{ij} < p_\epsilon^{ij}$ , the SC occurs from the high-pressure to the low-pressure phase, and the inequality  $p \leq p_\epsilon^{ij}$  is valid. Similar reasonings are applicable to eq 6.

To define the Odqvist parameter for each phase,  $q_i$ , when the Odqvist parameter for the mixture,  $q$ , is already defined, one would have to solve a very complex elastoplastic micro-mechanical problem. Currently, an analytical solution to such a problem is not available. To find the simplest noncontradictory solution, we assume

$$q_i/q_j = S_{ji}^{w_{ij}} \quad \text{and} \quad q = \sum_{k=1}^n c_k q_k \quad \text{where } S_{ji} := \sigma_{yj}/\sigma_{yi} \quad (7)$$

and  $\sigma_{yi}$  is the yield strength of  $i$ th phase. Let us prove that all  $w_{ij}$  are the same, i.e.,  $w_{ij} = w$  for all  $i$  and  $j$ . First,  $q_j/q_i = S_{ij}^{w_{ji}}$ ; from this equation, we obtain  $q_i/q_j = S_{ij}^{w_{ji}}$ , which after comparison with eq 7 results in  $w_{ij} = w_{ji}$ . Then,  $q_i/q_k = S_{ki}^{w_{ki}}$ ; dividing this equality by eq 7, we obtain  $q_j/q_k = S_{ki}^{w_{ki}} S_{ij}^{w_{ij}}$ . Since  $q_j/q_k = S_{kj}^{w_{kj}}$  is independent of  $\sigma_{yi}$  (see definition in eq 7),  $S_{ki}^{w_{ki}} S_{ij}^{w_{ij}} = S_{kj}^{w_{kj}}$  results in  $w_{ik} = w_{ij} = w_{jk}$ , which means that all  $w_{ij}$  are the same. It follows from eq 7 that

$$q_i = q \left( \sum_{k=1}^n c_k S_{ik}^{w_{ik}} \right)^{-1} \quad (8)$$

For SC with three phases, eq 8 simplifies to

$$\begin{aligned} q_1 &= q \frac{\sigma_{y2} \sigma_{y3}}{D} \\ q_2 &= q \frac{\sigma_{y1} \sigma_{y3}}{D} \\ q_3 &= q \frac{\sigma_{y1} \sigma_{y2}}{D} \end{aligned} \quad (9)$$

where  $D := c_1 \sigma_{y2} \sigma_{y3} + c_2 \sigma_{y1} \sigma_{y3} + c_3 \sigma_{y1} \sigma_{y2}$ . According to eq 8, with a stronger phase, the fraction of the equivalent strain concentrated within the phase is smaller; for  $\sigma_{y1} = \sigma_{y2} = \dots = \sigma_{yn}$ , one has  $q_1 = q_2 = \dots = q_n = q$ . As for  $\sigma_{yi} = (4-10)\sigma_{yk}$ ,  $q_i$  is negligible; the parameter  $w$  is estimated by  $w = (2-5)$ . Adding algebraically the rates of  $i \rightarrow k$  and  $k \rightarrow i$  SCs for all  $k \neq i$  and taking into account eq 8, one obtains the final system of kinetic equations

$$\frac{dc_i}{dq} = \sum_{k=1, k \neq i}^n \left[ \frac{\partial c_i}{\partial q_k} \frac{\partial q_k}{\partial q} H(\bar{p}_{ki}) - \frac{\partial c_k}{\partial q_i} \frac{\partial q_i}{\partial q} H(\bar{p}_{ik}) \right] \quad i = 1, \dots, n-1 \quad (10)$$

or in explicit form

$$\frac{dc_i}{dq} = \sum_{k=1, k \neq i}^n \left\{ \left[ \frac{c_k^{\xi_{ki}}}{\bar{p}_{ki}} H(\bar{p}_{ki}) \right]^{m_{ki}} \left( \sum_{m=1}^n c_m S_{km}^w \right)^{-1} \right\} - \left( \sum_{m=1}^n c_m S_{im}^w \right)^{-1} \sum_{k=1, k \neq i}^n \left[ \frac{c_i^{\xi_{ik}}}{\bar{p}_{ik}} H(\bar{p}_{ik}) \right]^{m_{ik}} \quad i = 1, \dots, n-1 \quad (11)$$

Natural constraint  $\sum_{k=1}^n c_k = 1$  has to be taken into account. To avoid  $i \rightarrow i$  SC, we assume  $a_{ii} \rightarrow \infty$  for each  $i$ .

Equation 11 is correct for strain-dominated kinetics. In the case of the pressure-dominated kinetics with  $\bar{p}_{ij} \geq 1$ , the phase  $i$  instantaneously transforms to the phase  $j$ , i.e.,  $c_i$  jumps to zero, and  $c_j$  has a jump by the value of  $c_i$  before the jump. In this case, the kinetic equation corresponding to phase  $i$  in eq 11 should not be used. The final kinetic equations (eq 11) have the following features that are significantly different from the classical chemical kinetic equation.

(a) The equations are derived from the equality of the driving forces for SCs to zero (i.e., from the thermodynamic condition) when nanoscale contribution to the driving force is properly taken into account.

(b) Time is not an independent parameter. Instead, plastic strain is a timelike parameter.

(c) Kinetics depends essentially on the mechanical properties of the phases, namely, on the ratio of the yield strengths.

(d) This dependence also involves volume fraction of the phases, which changes the order of the kinetic equations. Since the effect of each fraction cannot be presented in the form  $c_i^n$  with an exponent  $n$ , the order of the reaction is not determined.

(e) Kinetic parameters depend on pressure and two characteristic pressures for each SC as follows: (1) the pressure at which SC occurs under hydrostatic conditions, which takes into account the deviation of the actual SC pressure from the thermodynamic equilibrium pressure  $p_e^{ij}$  (determined by the equation  $p_e^{ij} \epsilon^{ij} - \Delta \psi_{ij} = 0$ ) due to irreversible processes (Note that the thermodynamic equilibrium pressure does not contribute to kinetic eq 11 and consequently cannot be determined from the results of strain-induced experiments. This is in contrast to the hope formulated in refs 12, 40, and 41 that plastic shear that reduces the pressure hysteresis allows for better localization of the thermodynamic equilibrium pressure.); (2) the minimal pressure  $p_e^{ij}$  for the SC from the low-pressure to the high-pressure phase (or maximum pressure  $p_e^{ij}$  for the SC from the high-pressure to the low-pressure phase) under which strain-induced SC can start at an infinitesimal rate.

**Stationary Solution.** Equation 11 has a number of parameters which makes it flexible to fit a wide range of experimentally observed kinetics. It is, however, reasonable to assume that the rate of each SC  $i \rightarrow j$  is proportional to  $c_i$  (again, because of the dependence of the term related to the yield strengths on  $c_k$ , this does not mean that we consider the first-order reaction). Indeed, the prescribed strain increment produces the prescribed value of defect densities, and the number of strain-induced nucleating defects in phase  $i$  is expected to be proportional to the volume of phase  $i$ , i.e., to  $c_i$ . For this case, we have  $\zeta_{ik} m_{ik} = 1$  for all  $i$  and  $k$ , and an analytical stationary solution to system of eq 11 can be found. For a three-phase system, within the pressure range of coexistence of all three phases (i.e., for  $0 \leq \bar{p}_{ij} \leq 1$  for all  $i$  and  $j$ ), the stationary solution has the following form:

$$\begin{aligned} c_1 &= \frac{B_1 \sigma_{y1}^w}{B} \\ c_2 &= \frac{B_2 \sigma_{y2}^w}{B} \\ c_3 &= \frac{B_3 \sigma_{y3}^w}{B} \end{aligned} \quad (12)$$

where

$$B = B_1 \sigma_{y1}^w + B_2 \sigma_{y2}^w + B_3 \sigma_{y3}^w \quad (13)$$

$$B_1 = \left( \frac{\bar{p}_{21}}{a_{21}} \right)^{m_{21}} \left( \frac{\bar{p}_{32}}{a_{32}} \right)^{m_{32}} + \left( \frac{\bar{p}_{31}}{a_{31}} \right)^{m_{31}} \left( \frac{\bar{p}_{21}}{a_{21}} \right)^{m_{21}} + \left( \frac{\bar{p}_{31}}{a_{31}} \right)^{m_{31}} \left( \frac{\bar{p}_{23}}{a_{23}} \right)^{m_{23}} \quad (14)$$

$$B_2 = \left( \frac{\bar{p}_{12}}{a_{12}} \right)^{m_{12}} \left( \frac{\bar{p}_{32}}{a_{32}} \right)^{m_{32}} + \left( \frac{\bar{p}_{13}}{a_{13}} \right)^{m_{13}} \left( \frac{\bar{p}_{32}}{a_{32}} \right)^{m_{32}} + \left( \frac{\bar{p}_{12}}{a_{12}} \right)^{m_{12}} \left( \frac{\bar{p}_{31}}{a_{31}} \right)^{m_{31}} \quad (15)$$

$$B_3 = \left( \frac{\bar{p}_{12}}{a_{12}} \right)^{m_{12}} \left( \frac{\bar{p}_{23}}{a_{23}} \right)^{m_{23}} + \left( \frac{\bar{p}_{13}}{a_{13}} \right)^{m_{13}} \left( \frac{\bar{p}_{21}}{a_{21}} \right)^{m_{21}} + \left( \frac{\bar{p}_{13}}{a_{13}} \right)^{m_{13}} \left( \frac{\bar{p}_{23}}{a_{23}} \right)^{m_{23}} \quad (16)$$

It is clear that  $\sum c_i = 1$ . Each  $B_i$  has contributions due to the following SCs: direct SCs to the phase  $i$ , ( $j \rightarrow i$ ) ( $k \rightarrow i$ ); indirect SCs to the phase  $i$  through another phase, ( $j \rightarrow k$ ) ( $k \rightarrow i$ ) and ( $k \rightarrow j$ ) ( $j \rightarrow i$ ); and SCs from the  $i$  phase ( $i \rightarrow j$ ) do not contribute. If all  $(1/a_{ik})^{m_{ik}}$  are the same, the stationary solution is independent of  $a_{ik}$ . An analysis of the three-phase case will be considered below for Si and Ge.

#### IV. Structural Changes Between Two Phases in an Inert Matrix

**Kinetic Equation.** Here, we consider the case when one of the three phases (for example, phase 3) does not participate in SC, i.e.,  $c_3 = \text{const}$ ; phase 1 and phase 2 are low- and high-pressure phases, respectively. Then, only one of the equations from eq 11 has to be considered, which can be presented in the following form

$$\frac{dc_2}{dq} = \frac{\left[ \frac{c_1^{\xi_{12}}}{a_{12}} \bar{p}_{12} H(\bar{p}_{12}) \right]^{m_{12}}}{c_1 S_{11}^w + c_2 S_{12}^w + c_3 S_{13}^w} - \frac{\left[ \frac{c_2^{\xi_{21}}}{a_{21}} \bar{p}_{21} H(\bar{p}_{21}) \right]^{m_{21}}}{c_1 S_{21}^w + c_2 S_{22}^w + c_3 S_{23}^w} \quad (17)$$

Consider the pressure–volumetric strain ( $\epsilon = 1 - v_2/v_1 \geq 0$ ) curve (Figure 3) under hydrostatic loading for  $p_h^{21} = \text{const}$  and  $p_h^{12} = \text{const}$ . For pressure-dominated kinetics, phase 1 is absolutely unstable and cannot exist for  $p > p_h^{12}$ ; similarly, phase 2 is absolutely unstable and cannot exist for  $p < p_h^{21}$ . For strain-dominated kinetics, phase 1 can exist for  $p > p_h^{12}$  and phase 2 can exist for  $p < p_h^{21}$ . For a volume fraction of the second phase in a 1 + 2 mixture,  $\bar{c}_2 := c_2/(1 - c_3)$ , one obtains  $\bar{c}_2 = AB/AC$ . Along line BD (unloading), there is no structural change. Strain-induced SC occurs under constant pressure due to plastic shear and can be visualized by the horizontal line, e.g., DE.

For an SC from the low-pressure to the high-pressure phase,  $p_e^{12} < p_h^{12}$ , since strain-induced SC starts at a lower pressure than under hydrostatic loading. For a SC from the high-pressure to the low-pressure phase, we obtain similarly that  $p_e^{21} > p_h^{21}$ . A

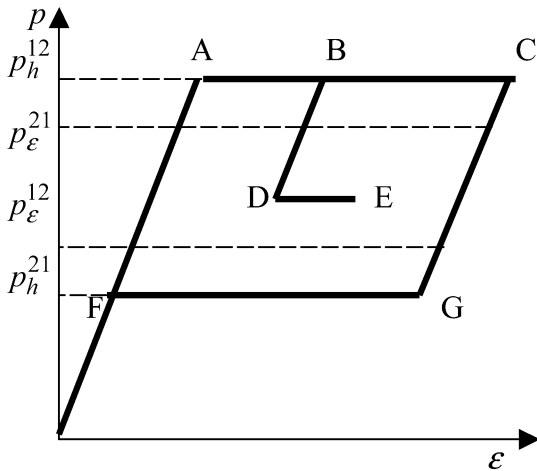


**Figure 3.** Pressure–volumetric strain curve under hydrostatic loading. SC 1 → 2 occurs along the line AC; SC 2 → 1 occurs along the line GF; the strain-induced SC under constant pressure takes place along line DE.

priori,  $p_\epsilon^{12}$  can be lower than  $p_h^{21}$  for strain-dominated kinetics. However, for pressure-dominated kinetics, if  $p_\epsilon^{12} < p_h^{21}$ , then for any pressure  $p$  in the range  $p_\epsilon^{12} < p < p_h^{21}$ , any amount of strain-induced phase 2 immediately transforms back to phase 1. This means that the pressure  $p_\epsilon^{12}$  has  $p_h^{21}$  as its lower limit, or  $p_h^{21} \leq p_\epsilon^{12}$ . Similarly, we may conclude that for pressure-dominated kinetics and SC from the high-pressure to the low-pressure phase:  $p_\epsilon^{21} \leq p_h^{12}$ .

There are two possible relations for pressures  $p_\epsilon^{12}$  and  $p_\epsilon^{21}$ :  $p_\epsilon^{12} > p_\epsilon^{21}$  and  $p_\epsilon^{12} < p_\epsilon^{21}$ .

(1) The case  $p_\epsilon^{12} > p_\epsilon^{21}$  corresponds to a weaker effect of strain on change in SC pressure. In this case, strain-induced SC cannot occur in the pressure range  $p_\epsilon^{21} < p < p_\epsilon^{12}$ , and volume fractions of phases remain constant and equal to their values obtained during pressure-induced SCs. Equation 17 simplifies to

$$\frac{dc_1}{dq} = \frac{\left(\frac{c_2^{\xi_{21}}}{a_{21}} \bar{p}_{21}\right)^{m_{21}}}{c_1 S_{21}^w + c_2 S_{22}^w + c_3 S_{23}^w} \quad \text{for } p < p_\epsilon^{21}$$

$$\frac{dc_2}{dq} = \frac{\left(\frac{c_1^{\xi_{12}}}{a_{12}} \bar{p}_{12}\right)^{m_{12}}}{c_1 S_{11}^w + c_2 S_{12}^w + c_3 S_{13}^w} \quad \text{for } p_\epsilon^{12} < p \quad (18)$$

The stationary solution for  $p < p_\epsilon^{21}$  is  $\bar{c}_1 = 1$  and for  $p_\epsilon^{12} < p$  is  $\bar{c}_2 = 1$ , since only one SC occurs in each of these pressure ranges (Figure 4).

Let us compare rates of SC for two cases:  $dc_1^I/dq$  for  $\sigma_{y1} = \sigma_{y3}$  and  $dc_1^{II}/dq$  for  $\sigma_{y1} \neq \sigma_{y3}$ . For  $c_1 > 0$ , we obtain the following:

$$\frac{dc_2^I}{dq} \frac{dc_2^{II}}{dq} = 1 + \frac{c_3(S_{13}^w - 1)}{(c_1 + c_3)(1 - S_{12}^w) + S_{12}^w} \quad (19)$$

Independent from  $S_{12}$ , it follows from eq 19 that if the yield strength of the inert matrix is greater (or smaller) than the yield strength of the parent phase,  $S_{13} < 1$  (or  $S_{13} > 1$ ), then SC II is accelerated (or decelerated) in comparison to SC I with  $\sigma_{y1} = \sigma_{y3}$ . This corresponds to experiments in refs 17 and 18. An

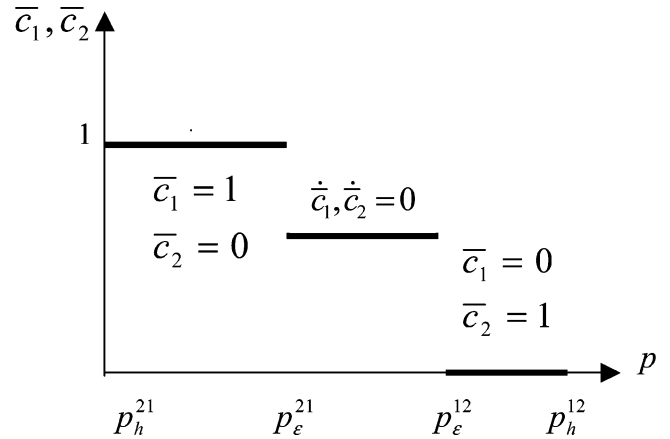


**Figure 4.** Stationary solutions for volume fractions for two-phase system in an inert matrix for the case  $p_\epsilon^{12} > p_\epsilon^{21}$ .

increase of  $c_3$  and decrease of  $S_{12}$  intensify this process. When  $\sigma_{y3} = \sigma_{y1}$ , addition of inert matrix does not affect SC, even if  $\sigma_{y3} > \sigma_{y2}$ . The analytical solutions of eqs 18 are

$$q = \frac{(1 - c_3)}{(\bar{p}_{21}/a_{21})^{m_{21}}} \frac{(S_{13}^w - S_{23}^w)}{S_{13}^w} \left( \frac{c_1}{(1 - c_3)} - \frac{1}{b_1} \log \left[ \frac{1 - c_3}{1 - c_3 - c_1} \right] \right) \quad \text{for } p < p_\epsilon^{21} \quad (20)$$

$$q = \frac{(1 - c_3)}{(\bar{p}_{12}/a_{12})^{m_{12}}} \frac{(S_{23}^w - S_{13}^w)}{S_{23}^w} \left( \frac{c_2}{(1 - c_3)} - \frac{1}{b_2} \log \left[ \frac{1 - c_3}{1 - c_3 - c_2} \right] \right) \quad \text{for } p_\epsilon^{12} < p \quad (21)$$

They can be inverted in the form

$$c_1 = (1 - c_3) \left\{ 1 + \frac{1}{b_1} \text{ProductLog} \left[ -b_1 \exp \left( -b_1 - q \frac{S_{13}^w (\bar{p}_{21}/a_{21})^{m_{21}}}{[1 + c_3(-1 + S_{13}^w)] S_{23}^w} \right) \right] \right\} \quad \text{for } p < p_\epsilon^{21} \quad (22)$$

$$c_2 = (1 - c_3) \left\{ 1 + \frac{1}{b_2} \text{ProductLog} \left[ -b_2 \exp \left( -b_2 - q \frac{S_{23}^w (\bar{p}_{12}/a_{12})^{m_{12}}}{[1 + c_3(-1 + S_{13}^w)] S_{13}^w} \right) \right] \right\} \quad \text{for } p_\epsilon^{12} < p \quad (23)$$

where  $\text{ProductLog}[z]$  gives the principal solution for  $y$  of the equation  $z = ye^{y^2}$ ,<sup>42</sup>

$$b_1 = \frac{(-1 + c_3)(S_{13}^w - S_{23}^w)}{[1 + c_3(-1 + S_{13}^w)] S_{23}^w}$$

and

$$b_2 = \frac{(-1 + c_3)(S_{13}^w - S_{23}^w)}{[1 + c_3(-1 + S_{13}^w)] S_{13}^w}$$

Figure 6 quantitatively supports our qualitative conclusion of

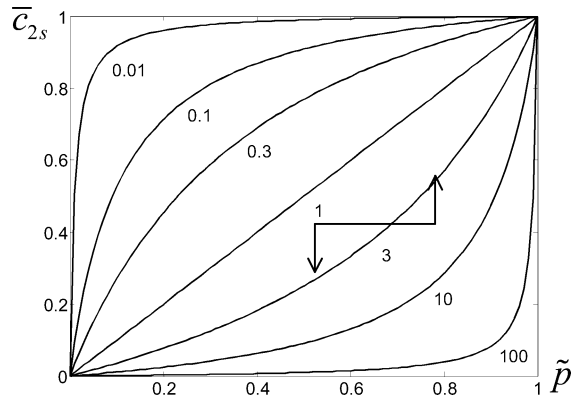


**Figure 5.** Relation between the stationary value of the volume fraction of the product phase 2 with respect to the mixture of phases 1 and 2 and the dimensionless pressure  $\tilde{p}$  for  $m_{ij} = \zeta_{ij} = 1$ . Phases 1 and 2 are deformed in an inert matrix and  $p_\epsilon^{12} < p_\epsilon^{21}$ . Numbers near curves designate values of  $M$ . If the material is under any pressure  $\tilde{p}$  and initial volume fraction of the phases correspond to a stationary state  $\bar{c}_{2s}$ , then any infinitesimal pressure increase (or decrease) followed by plastic straining will cause  $1 \rightarrow 2$  (or  $2 \rightarrow 1$ ) SC, i.e., pressure of direct and reverse SC differs infinitesimally, and pressure hysteresis is practically zero. This corresponds to the experiments in ref 11.

how the addition of an inert phase changes the rate of SC. Thus, adding a large amount of a strong inert phase could be used as a method of detection of a phase that cannot be revealed because of a low rate of SC. The dashed line in Figure 6 corresponds to the case with no inert phase. Note that the minimal hysteresis in SC pressure for strain-induced SC is determined by pressures  $p_\epsilon^{12}$  and  $p_\epsilon^{21}$ , and this hysteresis is smaller than the hysteresis  $p_h^{21} - p_h^{12}$  for pressure-induced SC. However, this does not help in localizing the phase equilibrium pressure  $p_e^{12}$ . There is no currently available information that would prove  $p_\epsilon^{12} < p_e^{12} < p_\epsilon^{21}$ ; instead, it may be that  $p_h^{21} < p_e^{12} < p_\epsilon^{12}$  or  $p_h^{12} > p_e^{21} > p_\epsilon^{21}$ .

(2) The opposite case,  $p_\epsilon^{12} < p_\epsilon^{21}$ , corresponds to a stronger effect of strain on the change in SC pressure. In the pressure ranges  $p_\epsilon^{21} < p$  and  $p > p_\epsilon^{12}$ , one of two SCs is possible, and eqs 18–23 derived for case 1 are valid. The stationary solution for  $p_\epsilon^{21} < p$  is  $c_{2s} = 1$  and for  $p > p_\epsilon^{12}$  is  $c_{2s} = 0$ . In the region  $p_\epsilon^{12} < p < p_\epsilon^{21}$ , both  $i \leftrightarrow j$  SCs are possible, and both terms in eq 17 are present. A stationary solution of eq 17 can be presented in the following form

$$\bar{c}_{2s} = \frac{1}{1 + M(1 - \tilde{p})^{1/\zeta_{21}}/\tilde{p}^{1/\zeta_{12}}} \quad (24)$$

where

$$M = (S_{12})^{w/g} \frac{a_{12}^{1/\zeta_{12}} (p_h^{12} - p_\epsilon^{12})^{1/\zeta_{12}}}{a_{21}^{1/\zeta_{21}} (p_\epsilon^{21} - p_h^{21})^{1/\zeta_{21}}} (p_\epsilon^{21} - p_\epsilon^{12})^{1/\zeta_{21} - 1/\zeta_{12}}$$

$$g = \zeta_{ij} m_{ij}$$

$$\tilde{p} = \frac{p - p_\epsilon^{12}}{p_\epsilon^{21} - p_\epsilon^{12}}$$

The stationary case of SC with two phases was solved in ref 30 for  $c_3 = 0$ . In the pressure range  $0 \leq \tilde{p} \leq 1$  (i.e., for  $p_\epsilon^{12} < p < p_\epsilon^{21}$ ),  $\bar{c}_{2s}$  varies from 0 to 1, and the shape of the  $\bar{c}_{2s}(\tilde{p})$  curve depends on the material parameters; see Figure 5. When  $p \rightarrow$

$p_\epsilon^{12}$ , one has  $\bar{c}_{2s} = 0$ ; when  $p \rightarrow p_\epsilon^{21}$ , one obtains  $\bar{c}_{2s} = 1$ . If, in particular,  $M = 1$  (e.g., for equal material parameters of both phases) and  $\zeta_{12} = \zeta_{21} = 1$ , then  $\bar{c}_{2s} = \tilde{p}$ . If  $M \rightarrow 0$  (e.g., if second phase is much stronger and/or  $a_{12}^{1/\zeta_{12}}/a_{21}^{1/\zeta_{21}} \rightarrow 0$ , i.e., kinetics of the high- to low-pressure SC is suppressed, and/or  $(p_\epsilon^{21} - p_\epsilon^{12})^{1/\zeta_{21} - 1/\zeta_{12}} (p_h^{12} - p_\epsilon^{12})^{1/\zeta_{12}} / (p_\epsilon^{21} - p_h^{21})^{1/\zeta_{21}} \rightarrow 0$ , then  $\bar{c}_{2s} = 1$ . In the opposite case  $M \rightarrow \infty$ ,  $\bar{c}_{2s} \rightarrow 0$ . If  $c < \bar{c}_{2s}$ , then direct SC will occur for straining under constant pressure  $p_\epsilon^{12} < p \leq p_\epsilon^{21}$ . In the opposite case, the reverse PT will take place. A number of conclusions can be made from analysis of eq 24 (see also ref 30), including the following:

(a) SC from the low- to the high-pressure phase is promoted by plastic deformation at a pressure above  $p_\epsilon^{12}$  only. This explains what may seem like a contradiction formulated in ref 43, namely, why large plastic deformation during the compression of materials (i.e., below  $p_\epsilon^{12}$ ) does not cause SC, yet relatively small shear strain at relatively high pressure significantly promotes SC.

(b) If  $M \gg 1$ , even if the initiation pressure for SC from low- to high-pressure phase can be reduced significantly, only a small amount of product phase can be produced at a pressure around  $p_\epsilon^{12}$  due to strain-induced nucleation. This is important for discovering a new phase but not for producing it. A significant amount of the high-pressure phase can be obtained under pressures around  $p_h^{12}$ , i.e., like for pressure-induced SC. A significant amount of the high-pressure phase can be induced by a large strain at a low pressure for  $M \ll 1$  only (Figure 5). One of the conditions for a small  $M$ ,  $(S_{21})^{1/g} \gg 1$ , shows that large plastic strains promote the appearance of hard phases more than weak phases. When this condition is fulfilled, then plastic flow localizes inside of phase 1 causing  $1 \rightarrow 2$  SC, while small plastic strain in phase 2 causes a small advance of the reverse SC.

(c) Zero-pressure hysteresis was observed at pressure  $p = 1.8$  GPa for B1  $\leftrightarrow$  B2 PT in KCl,<sup>11</sup> and it was assumed that this is an equilibrium pressure which can be used to plot a pressure-temperature phase diagram. However, if the initial state of material under any pressure  $p$  and the volume fraction of the phases corresponds to a stationary state  $\bar{c}_{2s}$ , then any infinitesimal pressure increase (or decrease) followed by plastic straining will cause  $1 \rightarrow 2$  ( $2 \rightarrow 1$ ) SC, i.e., pressure of direct and reverse SC differs infinitesimally and pressure hysteresis is practically zero (Figure 5). Since zero-pressure hysteresis can be obtained for any pressure in the range  $p_\epsilon^{12} < p < p_\epsilon^{21}$ , zero hysteresis definitely does not mean that the phase equilibrium pressure is found. Similar to case 1, the equilibrium pressure cannot be determined from a strain-induced experiment, because it does not contribute to any equation for strain-induced SCs.

(d) The inert phase does not change the stationary value of the volume fraction of the reacting phases with respect to the mixture of reacting phases. Equation 24 is valid for an  $n$ -phase system in any pressure range where only two phases undergo the SC. However, SC kinetics, especially at the initial stage, is significantly affected by the presence of an inert phase. Thus, for infinitesimal  $c_2$  and for  $\zeta_{ij} = m_{ij} = 1$ , eq 17 simplifies to

$$\frac{dc_2}{dq} = \left( \frac{c_1}{a_{12}} \bar{p}_{12} \right) \frac{1}{c_1 + c_3 S_{13}^w} \quad (25)$$

Equation 25 results in eq 19 with  $c_1 \approx 1 - c_3$ . Thus, the same conclusion is valid that the stronger (or weaker) the inert phase is with respect to the parent phase 1 the more SC is accelerated (or suppressed). Because acceleration occurs mostly at the initial

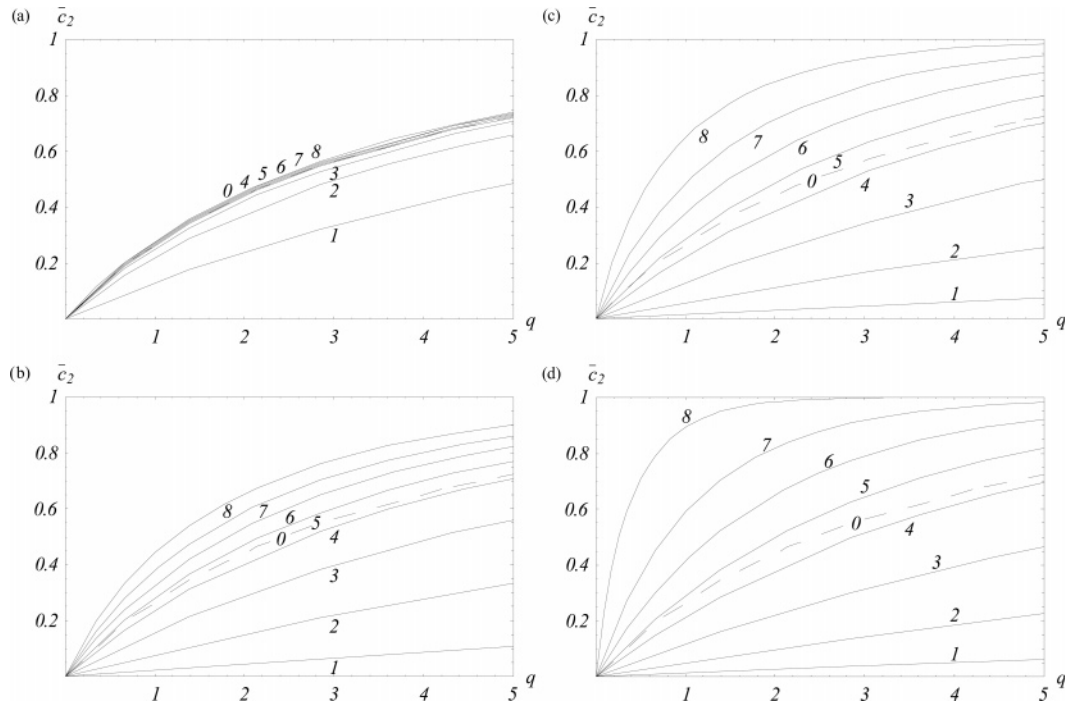


**Figure 6.** Change of the volume fraction of the phase 2,  $\bar{c}_2$ , with plastic strain,  $q$ , in the presence of an inert phase (when reverse SC does not occur) for  $p = 7.5$ ,  $p_e^{12} = 5.45$  GPa,  $p_h^{12} = 11.2$  GPa (parameters for Si), and  $S_{12} = 1.875$ ; 0,  $c_3 = 0$ , no inert phase; 1,  $S_{13} = 30$ ; 2,  $S_{13} = 7.5$ ; 3,  $S_{13} = 3$ ; 4,  $S_{13} = 1.5$ ; 5,  $S_{13} = 1$ ; 6,  $S_{13} = 0.6$ ; 7,  $S_{13} = 7$ ,  $S_{13} = 0.3$ ; 8,  $S_{13} = 0.0075$ . (a)  $c_3 = 0.05$ ; (b)  $c_3 = 0.5$ ; (c)  $c_3 = 0.75$ ; (d)  $c_3 = 0.9$ .

stage of SC, we can detect phases that otherwise could not be detected, potentially discovering new phases. Similarly, we can conclude that adding stronger particles to the material under study will facilitate SC and could cause SC which would not be obtained otherwise, e.g., metallic hydrogen.<sup>32–34</sup> Adding weaker particles will suppress SC, which is important, e.g., for explosives. Note that the above problem was considered in our papers<sup>28–31</sup> using a stationary solution for a two-phase model and some qualitative reasonings. It is clear that, for correct interpretation of the experiments in refs 17 and 18, a nonstationary solution for a three-phase model is necessary.

A nonstationary analytical solution to eq 17 can be found in the following inverse form:

$$q = \frac{a_{12}a_{21}}{X^2} \left( (1 - c_2 - c_3)A + B \log \frac{Y}{[Y + (1 - c_2 - c_3)X]} \right)$$

$$A = (S_{13}^w - S_{23}^w)X \quad B = X(1 - c_3 + c_3 S_{13}^w S_{23}^w)$$

$$X = (a_{12}\bar{p}_{21}S_{13}^w + a_{21}\bar{p}_{12}S_{23}^w) \quad Y = a_{12}(c_3 - 1)\bar{p}_{21}S_{13}^w \quad (26)$$

Figure 7 based on eq 26 illustrates the effect of the ratio of the yield strengths of the parent and inert phase and the concentration of the inert phase on the kinetics of SCs. The results are qualitatively the same as in the above case when only direct SC occurred. The only difference is that the stationary value (the same in all parts of Figure 7) is  $\bar{c}_{2s} < 1$ .

At the initial stage of deformation, Figures 6–7 demonstrate the linear relationship between volume fraction and plastic strain, which is observed for a number of CRs.<sup>17,18</sup>

## V. Phase Transformations in a Three-Phase System in Silicon and Germanium

**Phase Transformations in Si and Ge.** Silicon Si and germanium Ge represent extremely important materials because

of Si- and Ge-based electronics as well as their applications in solar cells and MEMS. PTs in Si and Ge are a subject of intensive basic and applied studies. One of the reasons is related to the variety of PTs, including martensitic, reconstructive, and crystal  $\leftrightarrow$  amorphous PT. Twelve crystalline and two amorphous phases of Si were revealed under different thermomechanical loadings. Understanding of strain-induced PTs in Si and Ge is of great practical importance. Information on stress and strain-induced PT in Si and Ge is crucial for understanding wear, friction, and erosion of Si and Ge. Some strain-induced high-pressure phases of Si and Ge are often observed in a machined surface of Si and Ge single crystals.<sup>44</sup> Machining of strong brittle semiconducting Si I and Ge I is accompanied by microcrack propagation inside the bulk materials. Utilizing strain-induced PTs into ductile metallic Si II or Ge II during machining allows one to realize and optimize the ductile regimes of machining.

There is a significant discrepancy in the phase behavior of Si and Ge reported in the literature. This discrepancy is related to the type of loading (hydrostatic pressure, nonhydrostatic pressure, or plastic straining), the preliminary plastic deformation (that changes the yield strength,  $K$ , and consequently  $p_h$ ), the initial structure (e.g., grain size), the size of the loading region (e.g., nanoindentation versus microindentation), and the loading rates. Since data for strain-induced PTs is available from refs 12, 13, and 45, we will rely on these refs for hydrostatic loadings as well. Also, since in refs 12 and 13 PTs between phases Si I, Si II, and Si III (and Ge I, Ge II, and Ge III) are studied, we will not consider in our equations the difference between bc8 Si III and the rhombohedral structure r8 Si XII or the difference between the diamond cubic structure Si I and the hexagonal diamond structure Si IV; both of these pairs have a small difference in specific volume. The crystal structure of Ge I and the  $\beta$ -tin structure of Ge II are similar to the structures of Si I and Si II, while Ge III has a simple tetragonal structure with twelve atoms per unit cell and is not similar to Si III. Some data taken from the recent review chapter<sup>46</sup> will be used as well.

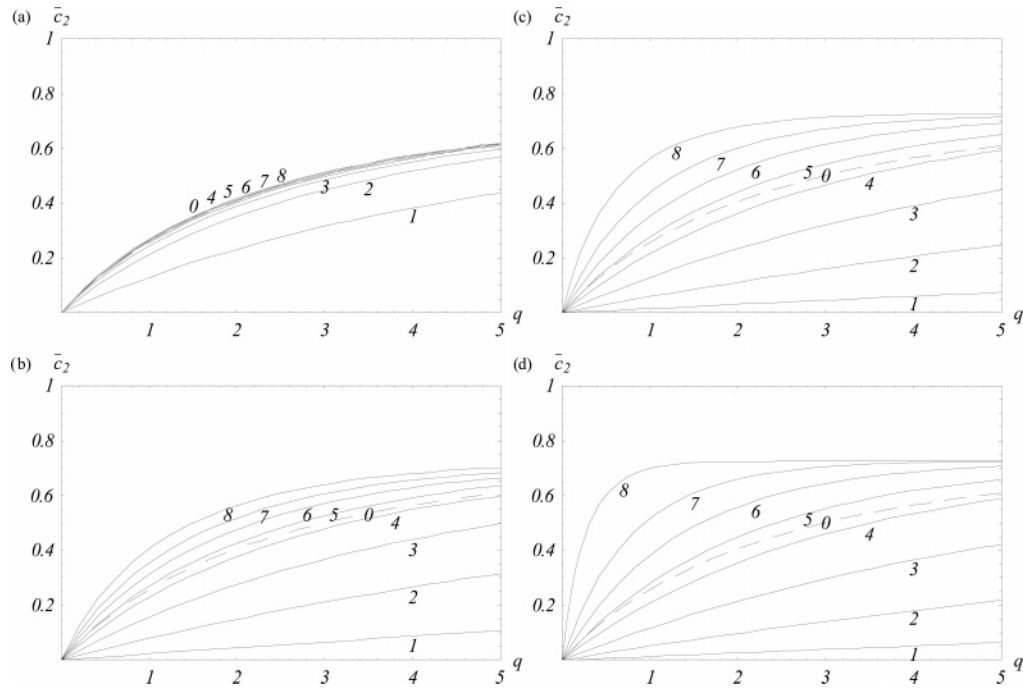


**Figure 7.** Change of the volume fraction of the phase 2,  $\bar{c}_2$ , with plastic strain,  $q$ , in the presence of an inert phase (when both direct and reverse PTs occur) for  $p = 7.5$ ,  $p_e^{12} = 5.45$  GPa,  $p_h^{12} = 11.2$  GPa, and  $p_e^{21} = 8$  GPa,  $p_h^{21} = 1$  GPa = (parameters for Si), and  $S_{12} = 1.875$ ; 0,  $c_3 = 0$ , no inert phase; 1,  $S_{13} = 30$ ; 2,  $S_{13} = 7.5$ ; 3,  $S_{13} = 3$ ; 4,  $S_{13} = 1.5$ ; 5,  $S_{13} = 1$ ; 6,  $S_{13} = 0.6$ ; 7,  $S_{13} = 0.3$ ; 8,  $S_{13} = 0.0075$ . (a)  $c_3 = 0.05$ ; (b)  $c_3 = 0.5$ ; (c)  $c_3 = 0.75$ ; (d)  $c_3 = 0.9$ .

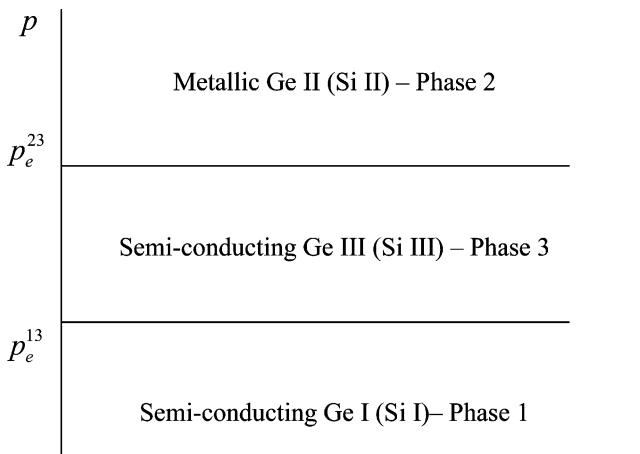


**Figure 8.** Equilibrium phase diagram for a three-phase system in Ge and Si.

**Hydrostatic Loading.** The equilibrium phase diagrams at room temperature for Ge and Si are shown in Figure 8 based on refs 12 and 13. We will consider the low-pressure semiconducting phase Si I (Ge I), the high-pressure semiconducting phase Si III (Ge III), and the high-pressure  $\beta$ -tin metallic phase Si II (Ge II). Here,  $p_e^{13} = 8.4$  GPa and  $p_e^{23} = 9.3$  GPa for Ge and  $p_e^{13} = 8.5$  GPa and  $p_e^{23} = 12.3$  GPa for Si.<sup>12,13</sup> The schematic pressure–volumetric strain diagram of the three-phase system under hydrostatic loading in Ge and Si is shown in Figure 9. During hydrostatic compression, Si I transforms at 9–16 GPa into a denser phase Si II, and Ge I starts transformation into Ge II at a pressure around 10 GPa.<sup>46</sup> Semiconducting phases Si III and Ge III are supposed to be stable within the pressure ranges 8.5–12.3 GPa and 8.4–9.3 GPa, respectively,<sup>12,13</sup> but they cannot be obtained under hydrostatic conditions during the pressure increase. Upon hydrostatic unloading, phases Ge II and Si II transform to Ge III and Si III, sometimes through intermediate phases (e.g., via Si IV<sup>45</sup> or Si XII<sup>46,47</sup>).

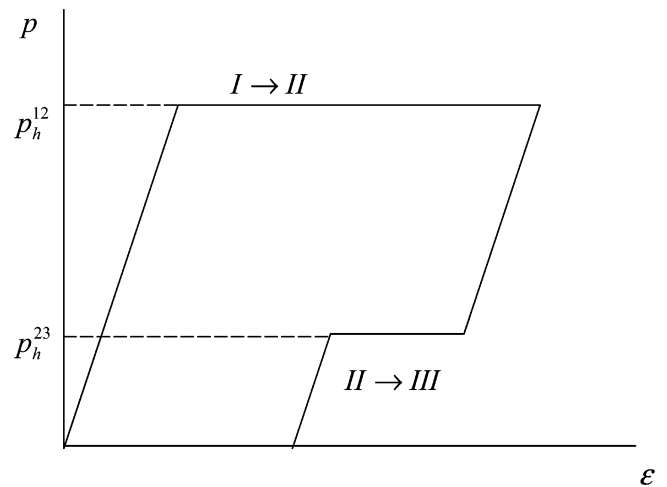


**Figure 9.** Pressure–volumetric strain curve under hydrostatic loading for a three-phase system in Ge and Si.

**Compression and Shear in a Rotational Diamond Anvil Cell.**<sup>12,13</sup> The following PTs are observed with an increase in rotation angle under a fixed axial force: Si I  $\rightarrow$  Si IV  $\rightarrow$  Si III at 3–4 GPa, and both Si I  $\rightarrow$  Si III  $\rightarrow$  Si II and Si I  $\rightarrow$  Si II at higher pressure (similar for Ge). Experiments show that the minimal pressure for Si I  $\rightarrow$  Si III (Ge I  $\rightarrow$  Ge III) PT under a very large plastic shear is  $p_e^{13} = 3.1$  GPa for Ge and  $p_e^{13} = 2.5$  GPa for Si. These values are significantly lower than the phase equilibrium pressures  $p_e^{13} = 8.4$  GPa for Ge and  $p_e^{13} = 8.5$  GPa for Si.<sup>12,13</sup> In addition, PT Si I  $\rightarrow$  Si II under shear was obtained at 5.45 GPa (for Ge at 4.9 GPa), which is lower than the pressure of 8.5 GPa required for reverse PT Si II  $\rightarrow$  Si III under hydrostatic conditions (for Ge at 7.6 GPa). These data should not, however, lead to the conclusion that the strain-induced phase II has to immediately undergo pressure-induced PT to phase III (this is not observed in experiments). The reason for such a paradoxical result is as follows: data under hydrostatic condi-

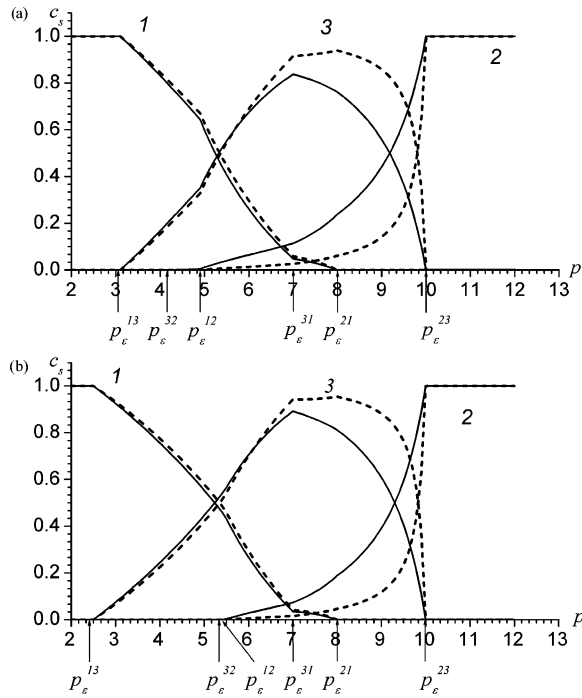


**Figure 10.** Stationary solution for the volume fractions of strain-induced phases vs pressure for SC in Ge (a) and Si (b).

tions are obtained without preliminary plastic deformation and strain hardening, while data for strain-induced PT are affected by large plastic straining. Large plastic straining increases the yield strength, and consequently,  $K = L\sigma_y\epsilon^{26,35}$  (where  $L$  is some coefficient) and  $|p_h - p_e| = K/\epsilon = L\sigma_y$ . For this reason, the difference  $|p_h^{23} - p_e^{23}|$  after plastic straining is much larger (and  $p_h^{23}$  is much lower) than without plastic straining and PT II  $\rightarrow$  III does not occur after strain-induced PT I  $\rightarrow$  II. A similar explanation may be used to justify why phase I transforms into the phase II, without first transforming into phase III (despite the fact that the equilibrium pressure  $p_e^{13} < p_e^{23}$ , Figure 8, and therefore, phase I should transform into phase III before phase II). The yield strength of the strong semiconducting phase III is much higher than that of the weak metallic phase II, which is why  $p_h^{13}$  is higher than  $p_h^{12}$ , and phase III cannot be obtained under hydrostatic loading. We will apply a three-phase model, Figure 2, and consider PTs among all three phases. We use the following values of characteristic pressures for Ge:

$$p_h^{13} = 18 \text{ GPa}, p_h^{32} = 20 \text{ GPa}, p_h^{21} = 1 \text{ GPa}, p_h^{31} = -0.5 \text{ GPa}, p_h^{23} = 3.5 \text{ GPa}, p_h^{12} = 10.5 \text{ GPa}, p_e^{13} = 3.1 \text{ GPa}, p_e^{32} = 4.2 \text{ GPa}, p_e^{21} = 8 \text{ GPa}, p_e^{31} = 7 \text{ GPa}, p_e^{23} = 10 \text{ GPa}, p_e^{12} = 4.9 \text{ GPa}$$

and for Si

$$p_h^{13} = 18 \text{ GPa}, p_h^{32} = 20 \text{ GPa}, p_h^{21} = 1 \text{ GPa}, p_h^{31} = -0.5 \text{ GPa}, p_h^{23} = 3.5 \text{ GPa}, p_h^{12} = 11.2 \text{ GPa}, p_e^{13} = 2.5 \text{ GPa}, p_e^{32} = 5.4 \text{ GPa}, p_e^{21} = 8 \text{ GPa}, p_e^{31} = 7 \text{ GPa}, p_e^{23} = 10 \text{ GPa}, p_e^{12} = 5.45 \text{ GPa}$$

Other parameters,  $a_{ij}$ ,  $m_{ij}$ , and  $w$ , are assumed to be 1. The equality  $a_{ij} = 1$  is equivalent to substituting  $q$  with  $q/a_{ij}$ . Some of these values ( $p_h^{12}$ ,  $p_e^{13}$ ,  $p_e^{32}$ , and  $p_e^{12}$ ) were taken from experimental data.<sup>12,13</sup> Some values for  $p_e^{21}$ ,  $p_e^{31}$ , and  $p_e^{23}$  are

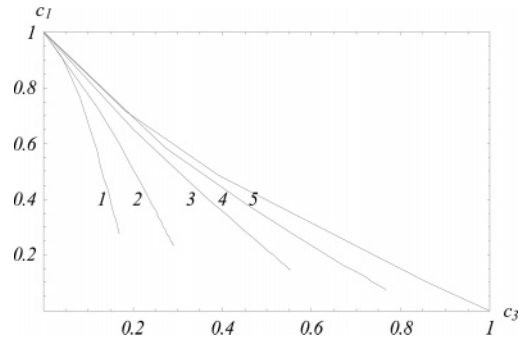


**Figure 11.** Function  $c_1$  ( $c_3$ ) for PT in Si, for  $p = 7$  GPa,  $S_{12} = 1.875:1$ ,  $S_{13} = 30$ ; 2,  $S_{13} = 15$ ; 3,  $S_{13} = 5$ ; 4,  $S_{13} = 1.875$ ; 5,  $S_{12} = 0.006$ .

given in refs 12 and 13, but since they are not the maximum values for the strain-induced PTs to low-pressure phases, we used larger numbers. The parameter  $p_h^{23}$  was taken to be lower than the experimentally observed value for the case without preliminary plastic deformation (see the above discussion on PT II  $\rightarrow$  III). Finally, parameters  $p_h^{13}$  and  $p_h^{32}$  are taken to be above the pressure range of interest and parameters  $p_h^{21}$  and  $p_h^{31}$  are taken to be below the observed PT pressure, because none of the above PTs occur under hydrostatic conditions.

**Stationary Solutions.** Stationary solutions for Ge and Si (eqs 12–16) are presented in Figure 10. The ratio of the yield stresses of the phases are unknown, especially when Ge and Si are under pressure and experience very large plastic deformations. It is known that semiconducting phases are significantly stronger than the metallic phase, and it can be assumed that the high-pressure (denser) semiconducting phase is stronger than the low-pressure semiconducting phase. Thus, we varied these parameters: solid lines in Figure 10 correspond to  $S_{31} = 1.33$  and  $S_{21} = 0.53$ , while dotted lines correspond to  $S_{31} = 1.20$  and  $S_{21} = 0.10$ . The curves in Figure 10 are interpreted as the result of the application of a very large shear under each chosen fixed pressure. In the general case, the pressure region is divided into three subregions. In the first subregion, there is only one phase. Thus, within the pressure range  $0 \leq p \leq p_e^{13}$  (below the pressure at which any strain-induced PT from phase 1 is possible, while all PTs to phase 1 can occur),  $c_{1s} = 1$ . Within the pressure range  $p \geq p_e^{23}$  (above the pressure at which any strain-induced PT from phase 2 can occur, while all PTs to phase 2 are possible),  $c_{2s} = 1$ . In the second subregion, two phases coexist. Within the pressure range  $p_e^{13} \leq p \leq p_e^{32}$ , shear leads to the increase of the fraction of phase 3 at the expense of phase 1. Similarly, for  $p_e^{21} \leq p \leq p_e^{23}$ , phase 3 appears from phase 2 with an increasing volume fraction and a decreasing pressure. The volume fractions of phases in two-phase regions are given by eq 24 with corresponding subscripts.

In the region  $p_e^{32} \leq p \leq p_e^{21}$ , all three phases coexist, and the volume fractions are given by eqs 12–16. It is clear from Figure 10 that there are jumps in the derivatives of the volume fraction curves at pressures  $p_e^{kl}$ , while characteristic hydrostatic pressures,  $p_h^{kl}$ , affect these curves in a continuous way.

In the pressure range  $p_e^{32} \leq p \leq p_e^{12}$ , phase 2 appears from phase 3, and PT  $1 \rightarrow 3 \rightarrow 2$  occurs with increasing  $c_{2s}$  and  $c_{3s}$ ; however,  $c_{2s}$  is very low. In the range  $p_e^{12} \leq p \leq p_e^{31}$ , direct PT  $1 \rightarrow 2$  also takes place. Both transformation paths ( $1 \rightarrow 3 \rightarrow 2$  at lower pressure and  $1 \rightarrow 2$  for higher pressure) have been observed experimentally,<sup>12,13</sup> while under hydrostatic pressure, phase 3 cannot be obtained from phase 1.

In the pressure range  $p_e^{31} \leq p \leq p_e^{21}$ , reverse PT of phase 3 into phase 1 is impossible. This leads to the disappearance of

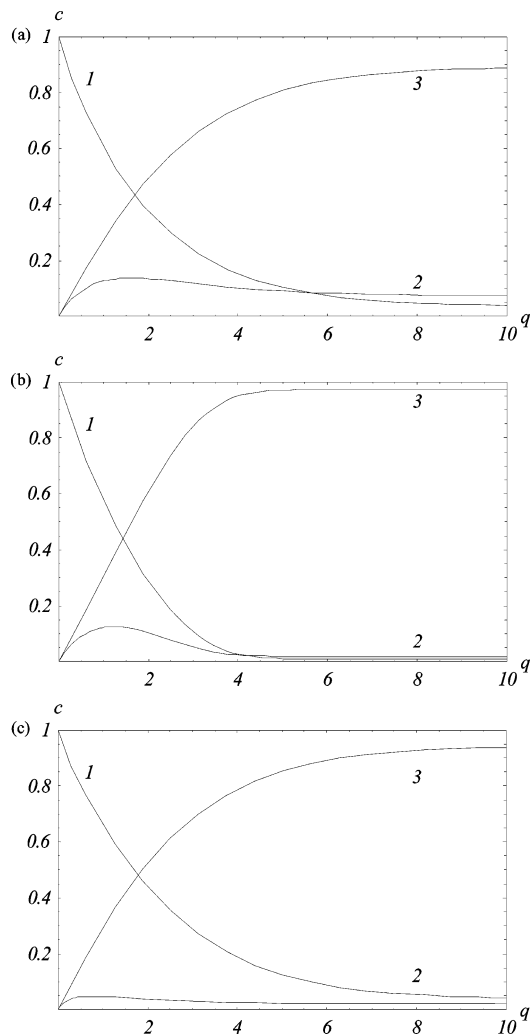


**Figure 12.** Change in volume fraction of three phases of Si during straining for  $p = 7$  GPa: (a)  $S_{31} = 1.333$ ,  $S_{21} = 0.533$ ; (b)  $S_{31} = 6.0$ ,  $S_{21} = 0.533$ ; (c)  $S_{31} = 1.333$ ,  $S_{21} = 0.133$ .

phase I at pressure  $p_{\epsilon}^{21}$  when reverse PT  $2 \rightarrow 1$  also ceases to occur. In addition, strain-induced PTs allow one to produce more than 90% of the Ge III (Si III) phases in the pressure range 7–8 GPa, while under hydrostatic conditions, the pressure has to reach a value that almost completes the  $I \rightarrow II$  PT (higher than 11 GPa), and then, phase III will appear after unloading.

Comparison of the dashed and solid lines in Figure 10 allows us to analyze the effects of the yield strength ratio. In these figures, the ratio  $S_{31}$  increases very little, while the ratio  $S_{21}$  increases by a factor of 5.3. The solid curve  $c_{1s}(p)$  lies slightly lower than the dotted curve, which is logical, since a larger strain is concentrated in phase I, and more of phase I transforms to phase III. A large increase in  $S_{21}$  strongly suppresses PT  $I \rightarrow II$ , and phase I transforms to phase III only.

**Transformation Kinetics.** Dividing the kinetic equation for  $dc_1/dq$  by the kinetic equation for  $dc_3/dq$ , we exclude strain  $q$  and obtain a differential equation for  $dc_1/dc_3$ . Figure 11 shows the numerical solution of this equation for various values of  $S_{ij}$  in the region where all three phases are present. Each curve presents all combinations between  $c_1$  and  $c_3$  that occur during plastic straining ( $c_2 = 1 - c_1 - c_3$ ). All curves end at the stationary values of  $c_1$  and  $c_3$ . With decreasing  $S_{13}$ , more of phase III appears during straining at the same value of  $c_1$ , both in the nonstationary and stationary regimes. For  $S_{13} = 0.075$ , the stationary value  $c_3 = 1$ .

To determine how the volume fraction of phases varies with the accumulated plastic strain, we solve the system of ordinary differential eq 11 numerically at some prescribed pressures. Results for  $p = 7$  GPa and three different combinations of the yield strengths of phases are presented in Figure 12. Stationary values obtained in Figure 12 coincide with the corresponding analytical solutions from eqs 12–16. Not only the stationary solutions but also the critical strain necessary to reach them depends on the ratio of the yield strengths of the phases. Thus, an increase of  $S_{31}$  from 1.333 to 6.0 reduces the critical strain from  $\sim 10$  to  $\sim 5$ . The volume fraction of the second phase passes through the maximum at relatively small strains for all cases under consideration. An important conclusion follows from Figure 12b. Despite the fact that the stationary value of phase II is very small and not detectable in the experiment, at the initial stage more than 10% of phase II was obtained. Consequently, if phase II would be unknown, to reveal it relatively small strains have to be applied. The same can be used for the search of new phases in other material systems.

## VI. Concluding Remarks

In this paper, a comprehensive conceptual approach to the kinetics of strain-induced SCs under high pressure is developed. Mechanism-based microscale kinetic equations for strain-induced SCs are derived. The main results are summarized in the Introduction.

Note that the current measurements of SC kinetics in both the rotational diamond and the Bridgman anvil cell<sup>17,18,48</sup> are only approximate. They have been related to the averaged pressure over the anvil, while the local pressure is heterogeneous and varies during the rotation. In particular, we believe that part of the promoting effect of the inert matrix with the larger yield strength is related to the pressure growth at the center of the sample while under a fixed averaged force.<sup>30,31</sup> In addition, plastic strain is determined mostly by the rotation of the anvil, which does not take into account relative sliding between the anvil and the material. Even if relative sliding is taken into account, another problem related to transformation-induced plasticity (see below) may lead to significant inaccuracy.

One of the possible ways to measure SC kinetics is developed in our recent papers<sup>20–22</sup> where PT from the graphite-like boron nitride BN to the superhard wurtzitic BN was studied. First, a method was developed to create an almost homogeneous pressure in the sample, which does not vary significantly during shear and PT. The pressure and the X-ray patterns were measured in situ locally along the radius of the sample for various rotation angles of the anvil. The volume fraction of the wurtzitic phase was evaluated using proper X-ray peaks. The key point we found is that the degree of disorder (concentration of turbostratic stacking faults,  $s$ ), which also was evaluated using proper X-ray peaks, is proportional to the plastic strain. That is why  $s$  can be used as a local measure of plastic strain. Using this approach, we found that, during the PT, actual plastic strain is 20 times larger than the value calculated by evaluating the rotation angle. The reason for such a huge plastic strain is that a large volumetric transformation strain, during any SC, creates significant internal stresses, which in combination with external nonhydrostatic stresses lead to additional plastic flow called transformation-induced plasticity. This demonstrates that using geometric measures of plastic strain (like rotation angle or shear strain) is not sufficient. Instead, one has to define and use a physical measure of plastic strain, similar to  $s$ . The density of different types of strain-induced defects, like dislocation density, twin density, and densities of slip bands and their intersection are all possible physical measures.

It is clear that the suggested kinetics is only the first approximation, and more complex relationships can be developed. One advancement may be made by taking into account strain hardening, i.e., dependence of  $\sigma_{yi}$  on  $q_i$ . Since strain hardening is different for different phases, it changes the kinetics. Strain hardening also suppresses SCs due to the equation  $K = L\sigma_y\epsilon$ .<sup>26,35</sup> growth in  $\sigma_y$  increases  $K$  and the deviation of the characteristic pressure,  $p_h$ , from the equilibrium pressure. This will complicate the analysis of stationary and nonstationary solutions. Fortunately, for large  $q$  ( $q > 1$  for metals and  $q > 0.4$  for rocks), strain hardening is saturated, and  $\sigma_{yi}$  is becoming strain-independent.<sup>37</sup>

**Acknowledgment.** The support of NSF (CMS-02011108 and CMS-0555909) and the ME Department of Texas Tech University is gratefully acknowledged.

## References and Notes

- (1) Koch, C. C. *Nanostruct. Mater.* **1993**, 2, 109.
- (2) Matteazzi, P.; Basset, D.; Miani, F.; Caer, G. Le. *Nanostruct. Mater.* **1993**, 2, 217.
- (3) Green, H. W.; Burnley, P. C. *Nature (London)* **1989**, 341, 773.
- (4) Kirby, S. W. *J. Geophys. Res.* **1987**, 92, 13789.
- (5) Wu, T. C.; Basset, W. A.; Burnley, P. C.; Weathers, M. S. *J. Geophys. Res.* **1993**, 98, 19767.
- (6) Boyle, V.; Frey, R.; Blake, O. Ninth Symposium (International) on Detonation I; OCNR; Aug. 28–Sept. 1, 1989, Portland, OR; 113291.
- (7) Coffey, C. S.; Sharma, J. *Proceedings of 11th International Detonation Symposium*; Snowmass Village, Colorado, 81615, 2001; p 751.
- (8) Levitas, V. I.; Nesterenko, V. F.; Meyers, M. A. *Acta Mater.* **1998**, 46, 5929.
- (9) Zhang, L. C.; Cheong, W. C. D. *High-Pressure Surface Science and Engineering*; Gogotsi, Y., Domnich, V., Eds.; Institute of Physics: Bristol, 2004; Chapter 2.2.
- (10) Bridgman, P. W. *Phys. Rev.* **1935**, 48, 825.
- (11) Blank, V. D.; Boguslavski, Yu. Ya.; Eremetz, M. I.; Izkevich, E. S.; Konyaev, Yu. S.; Shirokov, A. M.; Estrin, E. I. *JETP* **1984**, 87, 922.
- (12) Aleksandrova, M. M.; Blank, V. D.; Buga, S. G. *Solid State Phys.* **1993**, 35, 1308.
- (13) Blank, V. D.; Malyushitska, Z. H.; Kulnitskiy, B. A. *High Pressure Phys. Eng.* **1993**, 3, 28.
- (14) Serebryanaya, N. R.; Blank, V. D.; Ivdenko, V. A. *Phys. Lett. A* **1995**, 197, 63.
- (15) Batsanov, S. S.; Serebryanaya, N. R.; Blank, V. D.; Ivdenko, V. A. *Crystallogr. Rep.* **1995**, 40, 598.
- (16) Blank, V. D.; Popov, M.; Buga, S. G.; Davydov, V.; Denisov, V. N.; Ivlev, A. N.; Mavrin, B. N.; Agafonov, V.; Ceolin, R.; Szwarc, H.; Passat, A. *Phys. Lett. A* **1994**, 188, 281.
- (17) Zharov, A. *Usp. Khim.* **1984**, 53, 236.
- (18) Zharov, A. *High Pressure Chemistry and Physics of Polymers*; Kovarskii, Ed.; CRC Press: Boca Raton, 1994; Chapter 7.
- (19) Novikov, N.; Polotnyak, S.; Shvedov, L.; Levitas, V. *Superhard Mater.* **1999**, 3, 39.
- (20) Levitas, V. I.; Hashemi, J.; Ma, Y. *Europhys. Lett.* **2004**, 68, 1.
- (21) Levitas, V. I.; Ma, Y.; Hashemi, J. *Appl. Phys. Lett.* **2005**, 86, 071912.
- (22) Levitas, V. I.; Ma, Y.; Hashemi, J.; Holtz, M.; Guven N. *J. Chem. Phys.* In press.
- (23) Aleksandrova, M. M.; Blank, V. D.; Buga, S. G. *Solid State Phys.* **1993**, 35, 1308.
- (24) Gilman, J. J. *Philos. Mag. B* **1995**, 71, 1057.
- (25) Gilman, J. J. *Science* **1996**, 274, 65.
- (26) Levitas, V. I. *J. Mech. Phys. Solids* **1997**, 45, 923 and 1203.
- (27) Levitas, V. I.; Shvedov, L. K. *Phys. Rev. B* **2002**, 65, 1041091.
- (28) Levitas, V. I. *Europhys. Lett.* **2004**, 66, 687.
- (29) Levitas, V. I. *Phys. Lett. A* **2004**, 327, 180.
- (30) Levitas, V. I. *High-Pressure Surface Science and Engineering*; Gogotsi, Y., Domnich, V., Eds.; Institute of Physics: Bristol, 2004; Section 3.
- (31) Levitas, V. I. *Phys. Rev. B* **2004**, 70, 1.
- (32) Goncharov, A. F.; Gregoryanz, E.; Hemley, R. J.; Mao, H. K. *Proc. Natl. Acad. Sci. U.S.A.* **2001**, 98, 14234.
- (33) Loubeyre, P.; Occelli, F.; LeToullec, R. *Nature (London)* **2002**, 416, 613.
- (34) Narayana, C.; Luo, H.; Orloff, J.; Ruoff, A. L. *Nature (London)* **1998**, 393, 46.
- (35) Levitas, V. I. *Int. J. Sol. Struct.* **1998**, 35, 889.
- (36) Levitas, V. I. *Int. J. Plast.* **2000**, 16, 805 and 851.
- (37) Levitas, V. I. *Large Deformation of Materials with Complex Rheological Properties at Normal and High Pressure*; Nova Science Publishers: New York, 1996.
- (38) Blank, V. D.; Buga, S. G.; Serebryanaya, N. R.; Denisov, V. N.; Dubitsky, G. A.; Ivlev, A. N.; Mavrin, B. N.; Popov, M. Yu. *Phys. Lett. A* **1995**, 205, 208.
- (39) Levitas, V. I.; Idesman, A. V.; Olson, G. B. *Acta Mater.* **1999**, 47, 219.
- (40) Aleksandrova, M. M.; Blank, V. D.; Golobokov, A. E.; Konyaev, Yu. S.; Estrin, E. I. *Solid State Phys.* **1987**, 29, 2573.
- (41) Aleksandrova, M. M.; Blank, V. D.; Golobokov, A. E.; Konyaev, Yu. S. *Sov. Phys. Solid State* **1988**, 30, 577.
- (42) Wolfram, S. *The Mathematica Book*, 5th ed.; Wolfram Media: Champaign, IL, 2003.
- (43) Levitas, V. I. *J. Mech. Phys. Solids* **1997**, 45, 923 and 1203.
- (44) Patten, J. A.; Cherukuri, H.; Yan, J. *High-Pressure Surface Science and Engineering*; Gogotsi, Y., Domnich, V., Eds.; Institute of Physics: Bristol, 2004; Section 6.
- (45) Malyushitskaya, Z. V. *Inorganic Materials* **1999**, 35, 425.
- (46) Domnich, V.; Ge, D.; Gogotsi, Y. *High-Pressure Surface Science and Engineering*; Gogotsi, Y., Domnich, V., Eds.; Institute of Physics: Bristol, 2004; Chapter 5.1.
- (47) Blank, V. D.; Kulnitskiy, B. A. *High Pressure Res.* **1996**, 15, 31.
- (48) Aleksandrova, M. M.; Blank, V. D.; Golobokov, A. E.; Konyaev, Yu. S.; Estrin, E. I. *Solid State Phys.* **1987**, 29, 2573.